

Adaptive Compensation of Aerodynamic Effects during Takeoff and Landing Manoeuvres for a Scale Model Autonomous Helicopter

R. Mahony¹ and T. Hamel^{2,*}

¹Department of Electrical and Computer Systems Engineering, Monash University, Clayton, Victoria, 3800, Australia;
²Cemif, Université d'Evry, Université d'Evry, 40 rue du Pelvour, CE 1455, Courcouronnes, France

Control of a scale model autonomous helicopter during takeoff and landing manoeuvres has proved to be an extremely difficult problem. This is a consequence of the slowly time-varying and environment dependent nature of the aerodynamic forces encountered along with the high sensitivity of the helicopter to collective pitch changes during these manoeuvres. In this paper we propose a novel approach to the control problem for such manoeuvres. The proposed control design uses the motor torque rather than collective pitch as the principal control input and takes advantage of its reduced sensitivity to aerodynamic effects and structural properties to develop a parametric adaptive control algorithm that estimates the principal aerodynamic effects on-line.

Keywords: Autonomous helicopter; Extended matching; Nonlinear adaptive control

1. Introduction

There has been a growth of interest recently in the construction and control of scale model autonomous helicopters. The potential applications for such 'robotic' flying vehicles includes search and rescue missions, surveillance tasks, regular checks on the state of power lines, gas lines and fences over long distances and military applications, to mention just a few. A good understanding of the dynamic control problem for full scale

helicopters has been available for some time (cf. Prouty [22] based on linear control concepts. Some linear strategies for integrated control of scale model helicopters have been proposed [1,18,23,30,32] and have had a certain practical success. However, the high actuation to inertia ratios and highly nonlinear dynamics excited along desired flight trajectories for scale model autonomous helicopters have lead to the study of integrated nonlinear dynamic models for a scale model helicopter (cf. conference papers [2,3,14,16,25,26,31] and more recently the journal papers [24,27]). Much of the work done in this direction draws from earlier work on an idealised model of a VTOL aircraft [5,6,17,19,28]. However, to the authors knowledge, none of the existing work done using modern nonlinear control techniques for the helicopter or the VTOL deals with the changing aerodynamic effects that occur when an UAV approaches the ground. Coupled with the extreme sensitivity of a scale model helicopter to changes in collective pitch during such manoeuvres, the lack of aerodynamic modelling appears to have prevented the development of a robust control algorithm able to regulate takeoff and landing manoeuvres for a scale model autonomous helicopter. It is no simple matter to model *a priori* the aerodynamic effect that occur due to ground effects since they depend on the nature of the environment in which the helicopter is flying as well as ambient properties of the air. The authors know of no prior robust nonlinear control algorithm that deals with takeoff and landing manoeuvres for a scale model helicopter.

Correspondence and offprint requests to: Department of Electrical and Computer Systems Engineering, Monash University, Clayton, Victoria, 3800, Australia.
Email: mahony@ieee.org.

*Received December 1999; Accepted in revised form January 2001.
Recommended by J. Tsiniias and S. Bittani*

In this paper a novel approach to the control of a scale model helicopter for manoeuvres close to the ground is proposed. The nonlinear model popular in recent literature [2,3,14,25,26] is augmented by a simple aerodynamic model of thrust generated by the main rotor. This process introduces an additional dynamic state representing the rotor velocity and an additional input for the engine torque. The proposed control design uses the engine torque rather than the collective pitch as the principal input to control the main rotor thrust. Though this approach is unsuitable for other flight conditions it has several important advantages during landing and takeoff manoeuvres. Firstly, it overcomes the problems associated with the sensitivity of a scale model helicopter to collective pitch inputs during such manoeuvres. Secondly, the input required for takeoff and landing manoeuvres matches the final and initial phases of typical spin up and spin down phases for the main rotor for operation of a scale model autonomous helicopter. Lastly, and most importantly, the approach taken leads to a linear parametric representation of the unknown and time-varying main rotor lift coefficient that varies due to aerodynamic ground effects. To compensate for the varying lift coefficient encountered during the manoeuvres considered, an adaptive backstepping control design is proposed. The approach taken is equivalent to the tuning function approach proposed in [11]. It is simpler, however, to think of the design in terms of the extended matching techniques proposed in [21] coupled with the classical trick used in adaptive control to deal with unknown input gains (cf. for example [11, pp. 168–173]). The proposed control design provides a control Lyapunov function for the full system whose derivative is negative definite in the state errors. The structure of the equations lead to a strong

convergence result for all parametric errors under a weak boundedness condition on the desired trajectory. In practice, as long as some care is taken in choosing the adaptation gain, the robustness of the algorithm leads to an effective closed loop performance even in the presence of unmodelled dynamic perturbations and added input noise.

The paper is divided into five sections including the introduction. Section 2 presents the proposed model and motivates the use of engine torque as the principal thrust control. In Section 3 an adaptive control law is derived and a theorem is proved guaranteeing convergence of the tracking error and parameter estimates under certain unrestrictive assumptions. In Section 4 a series of simulations are presented that verify the performance of the adaptive controller under some simulated realistic perturbations. In Section 5 a brief resumé of the main contributions of the paper is presented.

2. A Dynamic Model of an Autonomous Helicopter

In this section a dynamic model of a scale model autonomous helicopter is presented.

Consider Fig. 1. Let $\mathcal{I} = \{E_x, E_y, E_z\}$ denote a right-hand inertial frame. Let the vector $\xi = (x, y, z)$ denote the position of the centre of mass of the helicopter relative to the frame \mathcal{I} . Let $\mathcal{A} = \{E_1^a, E_2^a, E_3^a\}$ be a (right-hand) body fixed frame for the helicopter. The orientation of the helicopter is given by a rotation $R: \mathcal{A} \rightarrow \mathcal{I}$, where $R \in SO(3)$ is an orthogonal rotation matrix. The angular velocity of airframe with respect to the body fixed frame is denoted Ω while the angular velocity of the rotor blades around axis

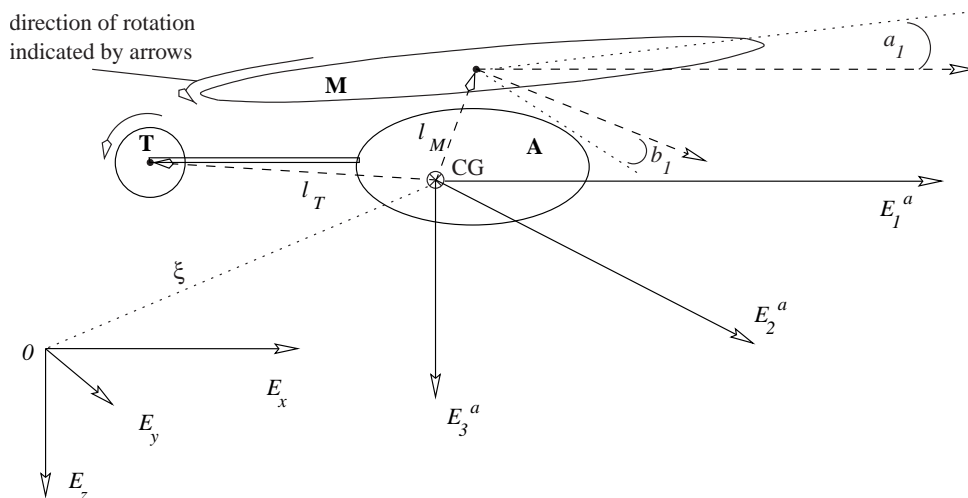


Fig. 1. Geometry of scale model autonomous helicopter.

of rotation is denoted ϖ . Note that the position of the rotor blades is irrelevant and only the angular velocity of the blades is considered.

Let $m \in \mathbb{R}$ denote the mass of the helicopter and $\mathbf{I} \in \mathbb{R}^{3 \times 3}$ denote the constant inertia matrix around the centre of mass (with respect to the body fixed frame \mathcal{A}). The dynamics of the helicopter airframe are modelled as rigid body motion [2,22,24]

$$\dot{\xi} = v, \quad (1)$$

$$m\dot{v} = F + mge_3 + \Sigma, \quad (2)$$

$$\dot{R} = Rsk(\Omega), \quad (3)$$

$$\mathbf{I}\dot{\Omega} = -\dot{\Omega} \times \mathbf{I}\Omega + \Gamma, \quad (4)$$

where $sk(\Omega)$ is the skew symmetric matrix associated with the vector product $\Omega \times u = sk(\Omega)u$. The vector $F \in \mathcal{I}$ combines the principal non-conservative forces applied to the helicopter airframe including main rotor thrust T and drag terms associated with the rotor wake on the airframe (cf. Eq. (10)). The term Σ denotes the modelling error in the linear force input and Γ denotes the external torque applied to the airframe. Some brief comments on the nature of these terms are given below. For a detailed discussion of helicopter aerodynamics the reader is referred to any standard text on helicopter design (cf. for example [22]).

Torque inputs Γ : Control input for the attitude dynamics is obtained via the tail rotor collective pitch and cyclic pitch input to the main rotor. Cyclic pitch inputs lead to a tilting of the rotor disk relative to the airframe and hence an inclination of the principal thrust component of the lift that, due to the offset between the rotor hub and centre of mass of the airframe, results in a torque input to the airframe attitude dynamics. The aerodynamic balance of the rotor disk is highly susceptible to local wind conditions and its tilting motion is strongly influenced by wind gusts and deformation of the rotor wake. Stabilisation of the attitude dynamics of a scale model autonomous helicopter (or indeed any helicopter) is a difficult problem. This is especially true when the helicopter enters the ground effect zone in which the rotor wake interacts with the earth's surface causing random wind gusts, the formation of vortices¹ and dynamic inflow resonance effects [4,20]. These complex aerodynamic disturbances tend to affect the roll and pitch stability of the helicopter first and lead to significant perturbation of the linear dynamics only if the motion of the helicopter tends towards instability. The stabilisation of

the attitude dynamics is not the subject of this paper and we assume that a suitable low level robust stabilising control is implemented that satisfactorily regulates the torque inputs Γ . The torque input τ_a used in the control design may be thought of as time-varying set point for the fast dynamics of the low level control. In the theoretical development we assume that $\Gamma = \tau_a$ in order to focus on the adaptive control algorithm. In Section 4 the robustness of the proposed algorithm is simulated with a noise-like disturbance added to the actual torque inputs $\Gamma = \tau_a + \nu(t)$. The disturbance ν is chosen to model the types of input disturbances that may be encountered due to the complex aerodynamic effects mentioned above.

Perturbation to the linear force input: Apart from some negligible noise effects the perturbation Σ incorporates an important dynamic coupling between the altitude and linear dynamics. The expression used in Section 4 (Eq. (59)) to model Σ for the robustness simulation corresponds to the form used in contemporary works [10,12,29]. The coupling leads to weakly non-minimum phase zero dynamics [10] that are qualitatively similar to those encountered for the original investigation of the VTOL [6]. Unlike the VTOL [17] the system is not differentially flat [12,15,29]. As a consequence (to the best of the authors knowledge) there is no control design available that deals with the full non-linear dynamics of the accepted model. The approach taken in prior control algorithms [2,3,16,25,26,31] is to design a robust controller for the system where $\Sigma \equiv 0$ and analyse the robustness of the closed loop system with respect to the perturbation Σ . We take an analogous approach in the present paper. The focus of the present investigation, however, is on robustness and adaptation with respect to inaccuracies in modelling the force F ; a different problem to that of robustness with respect to Σ , and not one that has been considered in previous work. For this reason, and in the interest of a less complicated presentation, we analyse only the dynamic model Eqs (1)–(4) where $\Sigma \equiv 0$, in detail and leave further discussion of the dynamic perturbation Σ until Section 4.

The dynamics of the main rotor disk around its axis of rotation is a decoupled system independent of its tilting motion. The torque exerted by the helicopter engine τ_e is transmitted via a flexible coupling to the rotor blades. The engine torque is opposed by an aerodynamic drag Q_M . The dynamic of the angular velocity of the disk is

$$\mathbf{I}_M \dot{\omega} = \tau_e - Q_M, \quad (5)$$

where \mathbf{I}_M is the moment of inertia of the rotor disk around its axis. Lead-lag motion of the rotor blades is negligible in this analysis.

¹A discussion of this effect is given in Prouty [22, p. 138] for the case of forward flight. Local wind and uneven ground can generate this situation in hover conditions.

The lift and drag generated by the main rotor is directly affected by two input controls: The *collective pitch* that is the angle of the rotor blades with respect to the plane of the rotor disk, controlled by regulating the elevation of the swash plate, and the velocity of the rotor blades, controlled by regulating the throttle to the engine. As a first approximation the total thrust T may be approximated as [22, p. 15]

$$T := C_\theta \varpi^2 (\theta - \phi), \quad (6)$$

where θ is the collective pitch and ϕ is the inflow angle generated by the down-flow of air present in all flight-conditions. The constant $C_\theta := (\rho r_M^3 n_M l_M a_M)/4$ combines respectively density of air, the cube of the radius of the rotor blades, the number of blades, the chord length of the blades and the lift constant linking angle of attack of the blade airfoil to the lift generated. The inflow angle may in general be approximated by

$$\phi \approx \tan(\phi) = \frac{v_M}{\varpi r_M},$$

where a small angle approximation is used for ‘tan’ v_M is the down-flow velocity at the main rotor while ϖr_M is the effective forward velocity of the rotor tip in the plane of the rotor disk. For hover condition in the absence of the ground effect the down-flow velocity v_M is itself related to the total thrust generated by the main rotor. Following Prouty [22, p. 4] one has

$$T = 2_\rho A_M v_M^2, \quad (7)$$

where A_M is the area of the rotor disk. Substituting into Eq. (6) yields

$$T := C_\theta \varpi^2 \theta - C_\phi \varpi \sqrt{T}, \quad (8)$$

where $C_\phi = C_\theta / (r_M \sqrt{2\rho A_M})$. In the presence of ground effect the actual down-flow velocity is computed as a ratio with respect to the clean air down-flow velocity based on experimentally validated data [22, p. 63–65]. The relationship between thrust and the clean air down-flow velocity is still a reasonable approximation in this situation and an expression for the actual thrust is obtained where C_ϕ varies with the height of the helicopter above the ground. Further discussion of the ground effect is deferred to Section 4.

Equation (8) poses considerable problems from a control perspective. The constants C_θ and C_ϕ are not precisely known and depend on variable factors such as the density of air, proximity to the ground, humidity and other factors. The relationship between the thrust generated and the collective pitch θ is nonlinear and depends on the angular velocity of the rotor. To overcome these difficulties we propose an alternative approach that exploits the rotor velocity as

the principal control input for the thrust T . Fix θ to be a constant value such that the thrust generated at the nominal operating condition supports the helicopter in hover. Dividing through Eq. (8) by ϖ^2 and completing the square for \sqrt{T}/ϖ one obtains

$$T = C_M \varpi^2, \quad (9)$$

where

$$C_M := \frac{4C_\theta^2 \theta^2}{\left(C_\phi + \sqrt{4C_\theta \theta + C_\phi^2}\right)^2},$$

may be thought of as an unknown parametric input uncertainty.

The total force applied to the airframe in direction E_3^a is (to a first approximation)

$$F = (T - D_M) E_3^a,$$

where $D_M = C_{D_M} \rho v_M^2$ [22, p. 7] is the drag due to the rotor wake on the helicopter airframe (C_{D_M} is the drag coefficient of the exposed airframe times its surface area). The drag is proportional to the thrust T due to the quadratic dependence on the down-flow velocity v_M (Eq. (7)); thus (noting that $E_3^a = Re_3$ one may write)

$$F := -b \varpi^2 (Re_3) \quad (10)$$

where $b > 0$ is an unknown parametric error. An important observation is that the sign of the constant b is known!

Recalling the discussion following the model Eqs (1)–(4) the aerodynamic torque inputs applied to the airframe using the cyclic and tail rotor control inputs are

$$\Gamma \approx \tau_a = (\tau_a^1, \tau_a^2, \tau_a^3).$$

Air resistance on both the rotors generate anti-torques applied to the airframe acting through the hub of the respective rotor (independent of the orientation of the actual rotor disk). With the collective pitch fixed to a constant value the air resistance on the main rotor blades is proportional to the square of the angular velocity of rotation of the rotor blades. Thus, one may write (cf. Eq. (5))

$$Q_M = d_M \varpi^2 E_3^a, \quad Q_T = d_T \varpi^2 E_2^a,$$

where d_M, d_T are unknown constants. The tail rotor and main rotor are mechanically coupled in all scale model autonomous helicopters resulting in the direct dependence of the tail rotor drag on ϖ^2 . The final torque contribution to the airframe dynamics comes from the reactive torque exerted on the airframe by the motor. This torque is equal and opposite to the engine torque applied to the main rotor dynamics.

Based on Eqs (1)–(4) and the above discussion the following approximate model is proposed

$$\dot{\xi} = v, \quad (11)$$

$$m\dot{v} = -b\varpi^2 Re_3 + mge_3, \quad (12)$$

$$R = Rsk(\Omega), \quad (13)$$

$$\mathbf{I}\dot{\Omega} = -\Omega \times \mathbf{I}\Omega - \tau_e e_3 - d_T \varpi^2 e_2 + \tau_a, \quad (14)$$

$$\mathbf{I}_M \dot{\varpi} = \tau_e - d_M \varpi^2, \quad (15)$$

where b , d_M and d_T are parametric uncertainties. There is a natural coupling between the rotor dynamics (Eq. (15)) and the yaw dynamics (third component of Eq. (14)). Indeed, if $\dot{\varpi} = 0$ then $\tau_e = d_M \varpi^2$ and substituting into Eq. (14) one obtains (a simplified form) of the classical equations for the motion of a helicopter [22, p. 557] [2,3,14,25,26,31].

3. Adaptive Control Design

In this section an adaptive control law is proposed for the helicopter model introduced in the previous section.

The problem considered is that of tracking a desired trajectory in the inertial frame \mathcal{I} . In particular, we consider a given trajectory $\hat{\xi}(t) = (\hat{x}(t), \hat{y}(t), \hat{z}(t))$ and look for a control law that achieves regulation of $|\xi - \hat{\xi}|$ to zero. In addition to the basic tracking problem it is desired that the control law estimate the unknown values b , d_M and d_T on-line. There are four physical inputs; the three torque components $\tau_a \in \mathbb{R}^3$ to the attitude dynamics, and a reactive torque τ_e , between the main rotors and the airframe, due to the engine. To ensure a well conditioned control algorithm a fourth objective is added to make the problem one of block input/output regulation. We choose to stabilise the yaw speed of the helicopter, that is the angular velocity around the axis E_3^a . This choice allows the helicopter to stabilise naturally to the most natural orientation with respect to the trajectory it is following.

Define the error

$$\delta_1 := \xi(t) - \hat{\xi}(t). \quad (16)$$

The derivative of δ_1 is given by

$$\dot{\delta}_1 = v - \hat{v}. \quad (17)$$

Define a first storage function:

$$S_1 = \frac{1}{2} |\delta_1|^2. \quad (18)$$

Taking the time derivative of S_1 and substituting for (11) yields

$$\frac{d}{dt} S_1 = \delta_1^T (v - \hat{v}). \quad (19)$$

Let v_d denote a desired value for the velocity v ; this is chosen such that the storage function S_1 is

monotonically decreasing when $v = v_d$,

$$v_d := \hat{v} - k_1 \delta_1. \quad (20)$$

With this choice one has

$$\dot{S}_1 = -k_1 |\delta_1|^2 + \frac{1}{m} \delta_1^T \delta_2, \quad (21)$$

where δ_2 defines the difference between the desired and true velocities and represents the new error used for the next step of the backstepping procedure.

$$\delta_2 := mv - mv_d. \quad (22)$$

Deriving δ_2 and recalling Eq. (12) yields

$$\dot{\delta}_2 = -b\varpi^2 Re_3 + mge_3 - m\dot{v}_d. \quad (23)$$

Following the standard trick in adaptive control when there is an unknown input gain, two new dynamic variables \hat{b} and $\hat{\rho}$, estimates of b and $\rho = 1/b$, are introduced. The estimate $\hat{\rho}$ is introduced to avoid the division by \hat{b} which may take value zero.

Analogous to previous work [3,14,25] the vector input $(\varpi^2 Re_3)$ is considered to be a vectorial virtual control. Considering the rotation matrix R and ϖ^2 as virtual controls, it is clear that vectorial virtual control chosen may be used to assign an arbitrary virtual input without encountering singularities.

Let $(\varpi^2 Re_3)_d$ denote the desired value of the vectorial virtual control and set

$$(\varpi^2 Re_3)_d = \hat{\rho} \left(mge_3 - m\dot{v}_d + k_2 \delta_2 + \frac{1}{m} \delta_1 \right) := \hat{\rho} X,$$

where $\hat{\rho}$ is the estimate of $\rho = 1/b$ and $X = mge_3 - m\dot{v}_d + k_2 \delta_2 + (1/m)\delta_1$. Note the desired values of ϖ and R are not uniquely defined by this equation, however, as long as the virtual control is preserved in its vectorial form (which is uniquely defined) this does not invalidate the backstepping procedure. The vectorial form is preserved until the final stage of backstepping when the structure of the Ω dynamics naturally leads to a decomposition of the control inputs. In this manner the control design avoids introducing singularities associated with an Euler coordinate representation of the rotation matrix! With the above choice of virtual control one has (cf. Eq. (23))

$$\dot{\delta}_2 = -b\hat{\rho}X + mge_3 - m\dot{v}_d + b(\hat{\rho}X - \varpi^2 Re_3).$$

The process of the backstepping continues by considering a third error

$$\delta_3 := \hat{\rho}X - \varpi^2 Re_3. \quad (24)$$

In terms of the error variables the δ_2 dynamics may now be written

$$\dot{\delta}_2 = -\frac{1}{m}\delta_1 - k_2\delta_2 + b\tilde{\rho}X + \hat{b}\delta_3 + \tilde{b}\delta_3, \quad (25)$$

where $\tilde{b} = b - \hat{b}$ and $\tilde{\rho} = 1/b - \hat{\rho}$.

Consider the storage function

$$S_2 = \frac{1}{2}|\delta_2|^2 + \frac{1}{2}bc_1\tilde{\rho}^2. \quad (26)$$

Since the unknown constant $b > 0$ is positive this storage function is positive definite in δ_2 and $\tilde{\rho}$. Deriving S_2 and substituting for Eq. (25) yields

$$\begin{aligned} \dot{S}_2 = & -\frac{1}{m}\delta_1^T\delta_2 - k_2|\delta_2|^2 + \hat{b}\delta_2^T\delta_3 \\ & + b\tilde{\rho}(\delta_2^T X - c_1\dot{\tilde{\rho}}) + \tilde{b}\delta_2^T\delta_3. \end{aligned} \quad (27)$$

Employing the standard trick in adaptive control to cancel the terms containing the unknown $\tilde{\rho}$ one chooses the following dynamics for $\hat{\rho}$

$$\dot{\hat{\rho}} = \frac{1}{c_1}\delta_2^T X. \quad (28)$$

Thus,

$$\dot{S}_2 = -\frac{1}{m}\delta_1^T\delta_2 - k_2|\delta_2|^2 + \hat{b}\delta_2^T\delta_3 + \tilde{b}\delta_2^T\delta_3. \quad (29)$$

For the third step of the procedure, consider the derivative of δ_3 and recall Eq. (13)

$$\dot{\delta}_3 = \dot{\hat{\rho}}X + \hat{\rho}\dot{X} - R(2\varpi\dot{\omega}e_3 + \varpi^2\text{sk}(\Omega)e_3). \quad (30)$$

To understand this equation it is necessary to express both the terms \dot{X} and $\dot{\omega}$ in more detail. Deriving \dot{X} and recalling Eqs (17), (20), (23) yields

$$\dot{X} = \dot{X}^m - (k_1 + k_2)\tilde{b}\varpi^2 Re_3, \quad (31)$$

where \dot{X}^m represents the known or measurable part of \dot{X} while the part depending on the unknown parametric error \tilde{b} must be dealt with separately in the control design. The measurable part of \dot{X} is given by

$$\begin{aligned} \dot{X}^m = & -m\ddot{\hat{v}} - (k_1 + k_2)(\hat{b}\varpi^2 Re_3 - mge_3) \\ & - k_1m\dot{\hat{v}} - k_2m\dot{v}_d + \frac{1}{m}(v - \hat{v}). \end{aligned}$$

To simplify the following analysis we rewrite Eq. (15)

$$\dot{\omega} = \frac{\tau_e}{\mathbf{I}_M} - \frac{d_M}{\mathbf{I}_M}\varpi^2 = w_e - d'_M\varpi^2, \quad (32)$$

where $d'_M = d_M/\mathbf{I}_M$ is an unknown constant and w_e is considered as the new input to the ϖ dynamics

Eq. (32). Since d'_M is unknown, an estimate \hat{d}'_M of d'_M is introduced and the parametric error is defined to be

$$\tilde{d}'_M = d'_M - \hat{d}'_M.$$

The δ_3 dynamics may be rewritten

$$\begin{aligned} \dot{\delta}_3 = & \dot{\hat{\rho}}X + \hat{\rho}\dot{X} + 2\varpi^3 d'_M Re_3 \\ & - R(2\varpi w_e e_3 + \varpi^2 \text{sk}(\Omega)e_3). \end{aligned}$$

The final term in this expression will act as the virtual control input for the next stage of the backstepping procedure.

Analogous to the procedure in the previous backstepping step the desired virtual control is assigned as a single vectorial equation

$$(2\varpi w_e e_3 + \varpi^2 \text{sk}(\Omega)e_3)_d := Y,$$

where

$$Y := R^T(\dot{\hat{\rho}}X + \hat{\rho}\dot{X}^m + \hat{b}\delta_2 + 2\varpi^3 \hat{d}'_M Re_3 + k_3\delta_3). \quad (33)$$

Note that the input w_e enters directly into the above expression for the desired vectorial virtual control. Assigning the control input w_e directly will introduce undesirable time-scale separation in the control action and reduces the robustness of the overall design when a general trajectory tracking control task is considered.

Remark 3.1. It should be noted that the control task considered for the popular control algorithms proposed by Hauser et al. [6] and Teel [28] for the VTOL do assign the height input directly. Such control designs act to stabilise the height of the airframe faster than the horizontal position and use the natural separation of the inputs to impose a time-scale separation within the system. The proposed approach assigns roughly equivalent dynamic response to all the state coordinates.

Consider a dynamic extension of the control w_e

$$\dot{\omega}_e = u. \quad (34)$$

Thus, the control input w_e becomes an internal variable of a dynamic controller and a new control input u is associated with the rotor dynamics.

Define a new error term

$$\delta_4 = Y - (2\varpi w_e e_3 + \varpi^2 \text{sk}(\Omega)e_3). \quad (35)$$

With the choice of virtual control (Eq. (33)) and the new error variable δ_4 , the δ_3 dynamics may be rewritten

$$\begin{aligned} \dot{\delta}_3 = & \dot{\hat{\rho}}X + \hat{\rho}\dot{X} + 2\varpi^3 \tilde{d}'_M Re_3 + 2\varpi^3 \hat{d}'_M Re_3 - RY + R\delta_4 \\ = & -\hat{b}\delta_2 - k_3\delta_3 + R\delta_4 - (k_1 + k_2)\tilde{b}\hat{\rho}\varpi^2 Re_3 \\ & + 2\varpi^3 \tilde{d}'_M Re_3. \end{aligned} \quad (36)$$

Thus, in addition to the standard backstepping structure there are two error terms associated with the unknown parametric errors \tilde{b} and \tilde{d}_M . These parametric error terms are in the correct form to be incorporated into the control design using extended matching adaptive control techniques in the next stage of the backstepping procedure.

The storage function associated with this stage of the computation is

$$S_3 = \frac{1}{2}|\delta_3|^2. \quad (37)$$

Taking the derivative of S_3 yields

$$\begin{aligned} \dot{S}_3 = & -\hat{b}\delta_3^T\delta_2 - k_3|\delta_3|^2 + \delta_3^T R\delta_4 \\ & - (k_1 + k_2)\hat{b}\hat{\rho}\varpi^2\delta_3^T R e_3 + 2\varpi^3\tilde{d}_M\delta_3^T R e_3. \end{aligned} \quad (38)$$

For the next and last stage for the backstepping, consider the derivative of δ_4

$$\dot{\delta}_4 = \dot{Y} - (2\dot{\varpi}\omega_e e_3 + 2\varpi\dot{u} + 2\varpi\dot{\omega}\text{sk}(\dot{\Omega})e_3 + \varpi^2\text{sk}(\dot{\Omega})e_3).$$

The δ_4 dynamics must be decomposed into a known part (or measurable part) and a part that depends on the parametric errors. In this case there are parametric errors associated with \tilde{b} and \tilde{d}_M . Standard but tedious calculations lead one to define

$$\begin{aligned} A = & -\text{sk}(\Omega)Y + R^T \left((\hat{\rho})^m X + 2\hat{\rho}\dot{X}^m + \hat{\rho}\frac{d}{dt}(X^m)^m \right. \\ & \left. + \hat{b}\delta_2 + \hat{b}\delta_2^m + k_3\delta_3^m \right) \\ & + R^T \left(6\varpi^2\hat{d}_M(\omega_e - \hat{d}_M\varpi^2) R e_3 - 2(\omega_e - \hat{d}_M\varpi^2) \right. \\ & \left. (\omega_e e_3 + \varpi\text{sk}(\Omega)e_3) + 2\varpi^3 e_3 \dot{\hat{d}}_M \right), \end{aligned} \quad (39)$$

$$\begin{aligned} B = & -\varpi^2(R e_3) \left(\left[X^T + (k_1 + k_2)\delta_2^T \right] X\hat{\rho}(k_1 + k_2) \right. \\ & \left. + \left(k_1k_2 + k_1k_3 + k_2k_3 + \frac{1}{m^2} \right) \hat{\rho} + \hat{b} \right), \end{aligned} \quad (40)$$

$$C = -6\varpi^4\hat{d}_M R_3 + 2\varpi^2(\omega_e e_3 + \varpi\text{sk}(\Omega)e_3). \quad (41)$$

In Eq. (39) the notation $(\hat{\rho})^m$, $(d/dt)(X^m)^m$, δ_2^m and δ_3^m denotes the known or measurable parts of $\hat{\rho}$, $(d/dt)(X^m)$, δ_2 and δ_3 respectively. The parts of these expressions that depend on the parametric errors \tilde{b} and \tilde{d}_M are included in the terms B and C in order that these errors are explicit in the expression for $\dot{\delta}_4$. Note that the expression for A depends on the dynamics \hat{b} and \hat{d}_M of the parametric estimates. These dynamics are not explicitly known at this stage of the procedure. The dynamics are assigned in the following analysis

and then back-substituted into the above expression in accordance with the usual practice of extended matching. With the above definitions the δ_4 dynamics may be written as

$$\begin{aligned} \dot{\delta}_4 = & A + \tilde{b}B + \tilde{d}_M C \\ & + (2\varpi\omega_e e_3 + \varpi^2\text{sk}(\dot{\Omega})e_3). \end{aligned} \quad (42)$$

At this point the control inputs u and τ_a may be utilised directly to terminate the backstepping procedure. The input τ_a is introduced via the derivative $\dot{\Omega}$. To simplify the following development a control input transformation of Eq. (14) is defined

$$w_a := \mathbf{I}^{-1} \left(-\Omega \times \mathbf{I}\Omega - {}_M w_e - \hat{d}_T \varpi^2 e_2 + \tau_a \right). \quad (43)$$

Since \mathbf{I} is full rank then this is certainly a bijective control input transformation between τ_a and w_a . With this choice

$$\dot{\Omega} = w_a + \hat{d}_T \varpi^2 \mathbf{I}^{-1} e_2.$$

Using the input transformation for τ_a , Eq. (42) may be rewritten

$$\begin{aligned} \dot{\delta}_4 = & A + \tilde{b}B + \tilde{d}_M C + \hat{d}_T D \\ & + (2\varpi\omega_e e_3 - \varpi^2\text{sk}(e_3)w_a), \end{aligned} \quad (44)$$

where

$$D = -\varpi^4\text{sk}(e_3)\mathbf{I}^{-1}e_2.$$

It is easily verified that

$$(2\varpi\omega_e e_3 - \varpi^2\text{sk}(e_3)w_a) = \begin{pmatrix} \varpi^2 w_a^2 \\ -\varpi^2 w_a^1 \\ 2\varpi u \end{pmatrix}. \quad (45)$$

Thus, as long as $\varpi \neq 0$ then full control of the δ_4 dynamics is available using only the inputs u , w_a^1 and w_a^2 . This leaves w_a^3 free to stabilise the yaw velocity.

The storage function associated with this stage of the backstepping is

$$S_4 = \frac{1}{2}|\delta_4|^2 + \frac{1}{2}c_2\tilde{b}^2 + \frac{1}{2}c_3\tilde{d}_M^2 + \frac{1}{2}c_4\tilde{d}_T^2.$$

Taking the derivative of S_4 yields

$$\begin{aligned} \dot{S}_4 = & \delta_4^T A + \tilde{b}\delta_4^T B + \tilde{d}_M\delta_4^T C + \hat{d}_T\delta_4^T D \\ & + \delta_4^T (2\varpi\omega_e e_3 - \varpi^2\text{sk}(e_3)w_a) \\ & - c_2\tilde{b}\dot{\tilde{b}} - c_3\tilde{d}_M\dot{\tilde{d}}_M - c_4\hat{d}_T\dot{\tilde{d}}_T \end{aligned} \quad (46)$$

From Eq. (46) it is clear how to choose the dynamics for \tilde{b} , \tilde{d}_M and \hat{d}_T to cancel the contributions of the

parametric errors \tilde{b} , \tilde{d}_M and \tilde{d}_T to the dynamics of S_4 . One chooses,

$$\dot{\hat{b}} = \frac{1}{c_2} (\delta_4^T B + \delta_2^T \delta_3 - (k_1 + k_2) \hat{\rho} \varpi^2 \delta_3^T R e_3), \quad (47)$$

$$\dot{\hat{d}}_M = \frac{1}{c_3} (\delta_4^T C + 2\varpi^3 \delta_3^T R e_3), \quad (48)$$

$$\dot{\hat{d}}_T = \frac{1}{c_4} \delta_4^T D. \quad (49)$$

The additional terms in Eqs (47)–(49) not associated with cancelling the contributions of the parametric errors in Eq. (46) cancel parametric errors arising in \dot{S}_3 and \dot{S}_4 (Eqs (29) and (38)).

The above dynamic expressions for \hat{b} and \hat{d}_M are back substituted into the expression for A (Eq. (39)). Finally, the backstepping procedure is terminated by choosing

$$\begin{pmatrix} \varpi^2 w_a^2 \\ -\varpi^2 w_a^1 \\ 2\varpi u \end{pmatrix} = -A - R^T \delta_3 - k_4 \delta_4. \quad (50)$$

With the choice of dynamics for the estimates \hat{b} , \hat{d}_M and \hat{d}_T (Eqs (47)–(49)) and the control inputs (u, w_a^1, w_a^2) Eq. (50) the derivative of S_4 may be rewritten

$$\begin{aligned} \dot{S}_4 &= -k_4 |\delta_4|^2 - \delta_4^T R^T \delta_3 \\ &\quad - \tilde{b} (\delta_2^T \delta_3 - (k_1 + k_2) \hat{\rho} \varpi^2 \delta_3^T R e_3) \\ &\quad - \tilde{d}_M (2\varpi^3 \delta_3^T R e_3). \end{aligned} \quad (51)$$

A function of the particular structure of the autonomous helicopter equations and the control strategy considered is that the backstepping procedure requires only the control inputs u , w_a^1 and w_a^2 to achieve the desired adaptive tracking of the trajectory $\hat{\xi}$. This leaves the input w_a^3 free to stabilise the yaw speed. Let

$$w_a^3 = -k_5 \Omega^3 \quad (52)$$

where $k_5 > 0$.

The proposed control algorithm achieves the monotonic decrease of the following Lyapunov function

$$\mathcal{L} = S_1 + S_2 + S_3 + S_4 + \frac{1}{2} (\Omega^3)^2.$$

This is easily verified by computing the derivative of \mathcal{L} and substituting for the expressions previously given for \dot{S}_1 , \dot{S}_2 , \dot{S}_3 and \dot{S}_4 (Eqs (21), (29), (38) and (51)). Cancelling the cross terms, it follows that

$$\begin{aligned} \dot{\mathcal{L}} &= -k_1 |\delta_1|^2 - k_2 |\delta_2|^2 - k_3 |\delta_3|^2 \\ &\quad - k_4 |\delta_4|^2 - k_5 (\Omega^3)^2. \end{aligned} \quad (53)$$

Theorem 3.2. Consider the dynamics defined by Eqs (11)–(15). Let the controls w_a and u be given by Eqs (50) and (25) and recover the control inputs w and τ_e from Eqs (43), (32) and (34). Then, for control laws for w_a and u , given by Eqs (45) and (52), well defined for all time (cf. Remark 3.3), the proposed control algorithm asymptotically stabilises the error posture for the complete system Eqs (11)–(15)

$$\delta_1 \rightarrow 0, \quad \Omega^3 \rightarrow 0.$$

In addition if the desired trajectory satisfies

$$|\dot{v}| < g, \quad (54)$$

then the proposed control algorithm ensures that

$$\tilde{b}, \tilde{d}_M, \tilde{d}_T \rightarrow 0.$$

Remark 3.3. In the statement of Theorem 3.2 it is required that the control laws remain well defined. This statement is necessary because of the nonlinear dependence of the control inputs on the angular velocity of the main rotor (Eq. (45)). Indeed, if one chooses an absurd desired trajectory or a very large initial tracking error then a transient for which the control is not well defined is theoretically possible. Neither of these situations will ever occur if the proposed control is implemented with a sensible trajectory planning algorithm.

Proof. Applying the standard Lyapunov argument using the inequality Eq. (53) one concludes that $(\delta_1, \delta_2, \delta_3, \delta_4, \Omega^3)$ are exponentially stable to zero as t tends to infinity.

To prove convergence of the parameter errors we appeal to LaSalle's principle. The invariant set is contained in the set defined by the conditions $\delta_i \equiv 0$ and $\Omega^3 \equiv 0$. Recalling Eqs (28) and (47)–(49) it follows that $\dot{\hat{\rho}} = 0$, $\dot{\hat{b}} = 0$, $\dot{\hat{d}}_M = 0$ and $\dot{\hat{d}}_T = 0$ on the invariant set. Consider the expression for the derivative of δ_2 (Eq. (25)) and note (Eq. (54)) that $X \neq 0$ on the invariant set. It follows that a further condition on the invariant set is $\tilde{\rho} = 0$, and consequently that $\hat{\rho}$ converges to its true value.

From the derivative of δ_3 (Eq. (36)), it follows that

$$(k_1 + k_2) \tilde{b} \hat{\rho} = 2\varpi \tilde{d}_M \quad (55)$$

on the invariant set. Note that on the invariant set \tilde{b} , \tilde{d}_M and $\hat{\rho} = \rho$ are constant and as a consequence either ϖ is constant or $\tilde{b} = 0$ and $\tilde{d}_M = 0$. In the case where the control design is used to track a persistently exciting trajectory then it is simple to show that ϖ must continue to vary (since it is directly linked to the control input) and the convergence of the parameter

estimates is proved. In the case where a stabilising manoeuvre is considered (e.g. a landing manoeuvre) then it is expected that $\varpi \rightarrow \varpi_\infty$ converges to a constant value. In this case it is sufficient to analyse the invariant trajectories for which $\dot{\varpi} = 0$ and use LaSalle's principle to show the only invariant trajectories satisfying the system dynamics are those for which the parametric errors are zero.

Consider the trajectories of the closed loop system for which $\dot{\varpi} = 0$, $\dot{\hat{\rho}} = 0$, $\dot{\hat{b}} = 0$, $\dot{\hat{d}}_M = 0$ and $\dot{\hat{\rho}} = \rho$. Then from Eq. (32) one has that $w_e = d'_M \varpi^2$. Substituting in the expression for δ_4 (Eq. (35)) one obtains

$$-\rho m R^T \ddot{\hat{v}} + 2\varpi^3 \tilde{d}_M e_3 - \varpi^2 \text{sk}(\Omega) e_3 = 0. \quad (56)$$

Multiplying the above expression by e_3^T , it follows that

$$-\rho m e_3^T R^T \ddot{\hat{v}} + 2\varpi^3 \tilde{d}_M = 0.$$

Therefore

$$2\varpi^3 \tilde{d}_M = \rho m (R e_3)^T \ddot{\hat{v}}. \quad (57)$$

Recalling the derivative of δ_2 (Eq. (23)), one has

$$R e_3 = \frac{m}{b\varpi^2} (g e_3 - \dot{\hat{v}}).$$

Substituting one obtains

$$\ddot{\hat{v}}^T (g e_3 - \dot{\hat{v}}) = \frac{2b\varpi^5 \tilde{d}_M}{\rho m^2} =: A_0,$$

where A_0 is a constant. The left hand side may be written as an exact derivative $(d/dt) \left(g \dot{\hat{v}}^T e_3 - (1/2) |\dot{\hat{v}}|^2 \right)$. Integrating both sides one obtains

$$\left(g \dot{\hat{v}}^T e_3 - \frac{1}{2} |\dot{\hat{v}}|^2 \right) = C_0 + A_0 t$$

for constant of integration c_0 . Note there is no need that C_0 or A_0 are positive, however, by completing the square and taking norms one obtains

$$|\dot{\hat{v}} - g e_3|^2 \geq |A_0| t - |C_0| - g^2. \quad (58)$$

As a consequence either $(\dot{\hat{v}} - g e_3) \rightarrow \infty$ or $|A_0| = 0$. The first case contradicts the assumption that $|\dot{\hat{v}}| < g$ and by inspecting the expression for A_0 it follows that on the invariant set $\tilde{d}_M = 0$. Recalling Eq. (55) it follows that \tilde{b} is also zero on the invariant set.

Finally, by inspecting the derivative of δ_4 (Eq. (44)) and replacing the control law (u, w_a) by its expression Eq. (50), it follows that $\tilde{d}_T = 0$ on the invariant set.

Applying LaSalle's principle to the closed loop system along with the bound on the acceleration of the desired trajectory proves asymptotic (not exponential) convergence of the parameter estimate to zero.

Remark 3.4. (i) There are only two places that the bound on the acceleration of the desired trajectory $|\dot{\hat{v}}| < g$ is used in the proof of Theorem 3.2. The first case is to show that $X \neq 0$ on the invariant set (Eq. (25)). This occurs if and only if $v_d = m g e_3$, or that the desired trajectory involves the helicopter dropping from the sky with zero lift applied. This is hardly a trajectory that is desirable in practice; nor is it one that requires a sophisticated control design to obtain. The second place that the condition is used is as an upper bound on the right hand side of Eq. (58). (ii) The argument used in the proof of Theorem 3.2 to prove convergence of the parameter errors to zero is based on LaSalle's principle. As a consequence, the proof given is not robust to perturbations in the system dynamics! However, as seen in Section 4 the parameter convergence is robust with respect to unmodelled dynamics and added noise. The reason for this can be seen if the argument applied in the proof is considered in detail. The conditions on the invariant set are derived as equalities based on the error dynamics of the system. If there are perturbations to these dynamics the equalities are only approximately true. However, even if only approximations are used the arguments used in the proof can be applied to provide bounds on the asymptotic parametric error. For example the constant A_0 is no longer a constant, however, it is slowly varying with time. The integral taken to obtain Eq. (58) may still be taken and the condition $A_0 \approx 0$ is obtained. Since Eq. (55) is also approximately true then this provides a bound on \tilde{b} in the limit. The details of a full robustness analysis is beyond the scope of this paper.

4. Simulation Results

In this section, a simulation example concerning a helicopter performing a landing manoeuvre is analysed.

The idealised model Eqs (11)–(15) proposed for the dynamics of a scale model helicopter is at best an approximation of actual system dynamics. Apart from general aerodynamic modelling errors, there are three main causes of errors in the model used: Firstly the time-variation of the parametric constants b , d_M and d_T encountered in practice during a landing or takeoff manoeuvre break the assumptions of the control design and will introduce tracking errors into the adaptive dynamics. Secondly, the dynamic perturbation Σ (Eq. (59)) is non-zero resulting in direct coupling of the roll (pitch) dynamics with latitudinal (longitudinal) linear dynamics. Lastly, the swirling winds encountered due to the interaction of the rotor wake with the ground tend to get sucked into the rotor inflow leading

to vortex and dynamic inflow effects [4,20], and bursts of noisy perturbations to the torque control inputs. The best performance that can be expected is a practical stabilisation of the system to a neighbourhood of the desired trajectory.

Two modifications of the proposed design may be undertaken to improve robustness of the closed loop design. To improve robustness of the adaptation process it is a good idea to add an additional σ -modification [7] to the estimator dynamics. The details are standard and are omitted. A second manner in which to improve the performance of the closed loop system is to implement the control design in tandem with a trajectory planning algorithm that takes into account trajectory initialisation issues [9] 11, pp. 162–164]. Implementing either of these modifications in the following simulations will tend to obscure the robustness properties of the control design with respect to unmeasured errors. For this reason we have opted to simulate the core algorithm and demonstrate its robustness subject to (simulated) real world disturbances. The performance of the closed loop system without σ -modification or trajectory initialisation is satisfactory even when time-varying parametric errors, significant unmodelled dynamics and noise are added. This confirms the robustness margin of the proposed algorithm.

The manoeuvre considered is a typical landing manoeuvre. As the helicopter enters the ground effect zone, the ratio of actual down-flow velocity to the clean air down-flow velocity decreases and the value of the parametric constant b increases. An approximation of the down-flow velocity ratio based on a piecewise linear approximation of Figure 1.41 [22, pp. 66] was used. Recalling Eq. (9) one may write an expression for the thrust T where C_M varies as

$$C_M := \frac{4C_\theta^2\theta^2}{\left(C_\phi \frac{v_M}{v_M^0} + \sqrt{4C_\theta\theta + C_\phi^2 \left(\frac{v_M}{v_M^0}\right)^2}\right)^2}.$$

The drag D_M also varies with the reduction in v_M with a ratio $D_M \approx C_{D_M}(v_M/v_M^0)^2(v_M^0)^2$. Combining these relationships along with the empirical dependence of v_M/v_M^0 on z/D one obtains the relationship $b := b(z/D)$ shown in Fig. 2.

The parameters for the helicopter used are based on preliminary modelling of the VARIO 23 cc radio controlled helicopter at the Université de Technologie de Compiègne. The parameters used are given in Table 1.

The control design used the following gains,

$$k_1 = 0.625, k_2 = 1, k_3 = 3, k_4 = 3, k_5 = 10, \\ c_1 = 3000, c_2 = 6000, c_3 = 8000, c_4 = 8000.$$

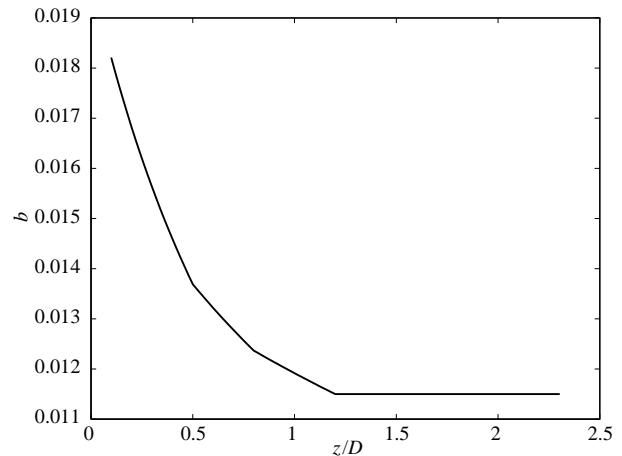


Fig. 2. Piecewise differentiable approximation of the parametric constant b as a function of height above the ground z/D normalised with respect to rotor diameter.

Table 1

Parameter	Value
m	9.6 kg
I_1^a	0.4 kg m ²
I_2^a	0.56 kg m ²
I_3^a	0.29 kg m ²
g	9.80 m s ⁻²
b	0.0115
d_M	0.001
d_T	0.0005

The gains for the adaptation dynamics must be chosen carefully since the relative scale of the parametric constants $\{|b|, |d_M|, |d_T|\}$ is roughly 10^{-3} of the errors associated with the states $\{|x|, |y|, |z|\}$. In addition the extended matching (or tuning function) approach leads to an adaptive algorithm with highly coupled dynamics. The approximation used for the dependence of b on the height is only piecewise differentiable and the effect of the impulse changes in slope appear to cause sharp disturbances in the closed loop system. This is particularly the case when the unmodelled dynamics due to the small body forces are included in the simulation. These dynamics couple the torque inputs (in which the higher derivatives of the adaptation dynamics are present) to the force inputs, and consequently remove the natural filtering effect of the system dynamics. It is possible that an adaptive backstepping design [8] (cf. also [11, Ch. 3]) might reduce sensitivity to these error dynamics at the expense of increasing the dynamic stiffness of the closed loop nonlinear system (due to the additional dynamic states in the control design). This poses the question of whether there is still a place for the early form of the adaptive backstepping design when a system shows

high sensitivity to changes in parametric error. In the present paper satisfactory performance was obtained using the proposed design.

The landing trajectory is generated as a stabilisation problem. Initially, the helicopter is assumed to be in hover some distance above the ground with the rotor speed corresponding to the necessary force to maintain stationary flight $b\omega^2 = gm \approx 94$. The desired trajectory chosen is the stationary point at $(0, 0, -0.25)$ corresponding to the helicopter touching ground (note the helicopter undercarriage is below the centre of mass by 25 cm). As a consequence the initial error in the Lyapunov system is large (none of the higher derivatives are matched) and the initial disturbance to parameter estimates trajectories are significant. The fact that the algorithm is well behaved under these circumstances shows its practical robustness.

The comparative control algorithm with no adaptation was obtained by setting the adaptation dynamics to zero and using estimates of the parametric constants. The estimates chosen were

$$\begin{aligned}\hat{b}_0 &:= 0.0109 \approx 0.95b, \\ \hat{\rho}_0 &:= \frac{1}{b_0}, \\ (\hat{d}_M)_0 &:= 0.002 \approx 2d_M, \\ (\hat{d}_T)_0 &:= 0.0003 \approx 0.6d_T.\end{aligned}$$

The key estimate is that corresponding to the lift coefficient b . In the case where a good estimate of b is available it is expected that a non-adaptive control design will outperform the proposed adaptive algorithm. Simulations indicate that until one enters the ground effect this is the case and in practice, the proposed adaptive algorithm should only be used in the situations for which it has been designed. In contrast the non-adaptive algorithm fails to achieve a successful landing manoeuvre due to increased lift encountered due to the unmodelled ground effect and leaves the helicopter hovering in the most dangerous and difficult zone of flight. To the authors knowledge, several teams working on the scale model autonomous helicopters have encountered problems of this nature. A common solution appears to be to turn the motor off and let gravity finish the landing manoeuvre. The authors hope that the present investigation will lead to a better solution in the long term. The system is not highly sensitive to errors in d_M and d_T larger parametric errors have been chosen for these estimates.

For simulation results, the classical ‘yaw’, ‘pitch’ and ‘roll’ Euler angles (ϕ, θ, ψ) favoured in aeronautical

applications are used to express the attitude of the airframe. In Fig. 3 the performance of the algorithm in the ideal case is shown. The initial position of the helicopter is $\xi_0 = (1, 2, -4)$ and its final position is $\xi_f = (0, 0, -0.25)$. In this case a constant parametric constant b is used and no unmodelled disturbances are present. Regarding Fig. 3, it is clear that the proposed control design functions perfectly and provides asymptotically stable convergence of system state and parametric error estimates.

In Fig. 4 the landing manoeuvre is simulated for both the non-adaptive (left) and adaptive (right) algorithms for the case where the ground effect is added. Note that the changing lift coefficient along with the dynamics of the system cause the helicopter to bounce as if on a cushion of air as it comes in to land (one clear bounce is visible in both cases in the trace of the z -coordinate of the centre plot). In the case of the non-adaptive design this effect is unavoidable and the helicopter will continue to bounce around on its ground effect air cushion until some modification to the control is made. For the adaptive control algorithm the initial bouncing effect is measurably reduced and the following transient shows little or no effect from the changing system parameters. The slight bounce that does occur for the adaptive system is due to the transient in the parameter estimates generated by the lack of trajectory initialisation. The gains c_1, \dots, c_4 were chosen to give the parameter estimates a convergence that is roughly twice as fast as the system dynamics (compare the convergence shown in Fig. 6 with that in Figs 4 or 5). In all the simulations shown, the parameter transients have died out after approximately 7 s and the landing manoeuvre is completed after approximately 15 s. The system dynamics from 7–15 s show no tendency towards instability even though the changes in ground effect are more severe close to the ground than those encountered during the first seven seconds (cf. Fig. 2).

Finally, a semi-realistic simulation is given for a landing manoeuvre. In addition to the changing ground effect the dynamic perturbation Σ is included and a noise like disturbance to the torque control is added. The form of Σ used is based on preliminary modelling of the VARIO 23 cc radio controlled helicopter at the Université de Technologie de Compiègne

$$R^T \Sigma = \begin{pmatrix} 0 & -2.2 & 0 \\ 2.2 & 0 & -0.7 \\ 0 & 0 & 0 \end{pmatrix} \begin{pmatrix} \Gamma^1 \\ \Gamma^2 \\ \Gamma^3 \end{pmatrix}, \quad (59)$$

where the factor of R^T transforms the expression into the body fixed frame [14]. The coupling between the

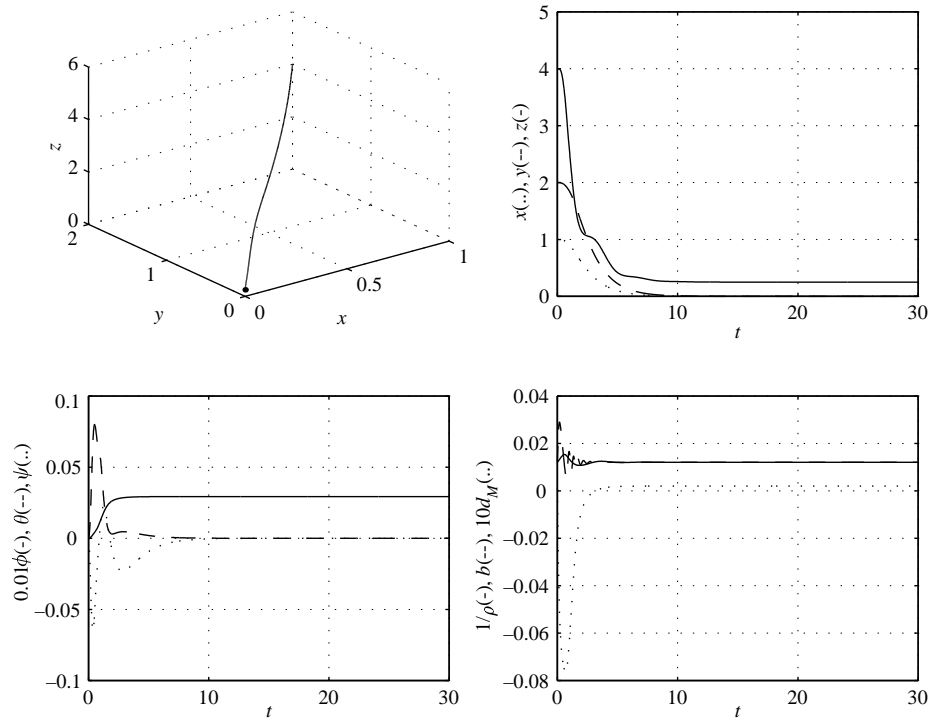


Fig. 3. Evolution of the system states and parameter estimates for the proposed closed loop system in the ideal case where all assumptions are satisfied.

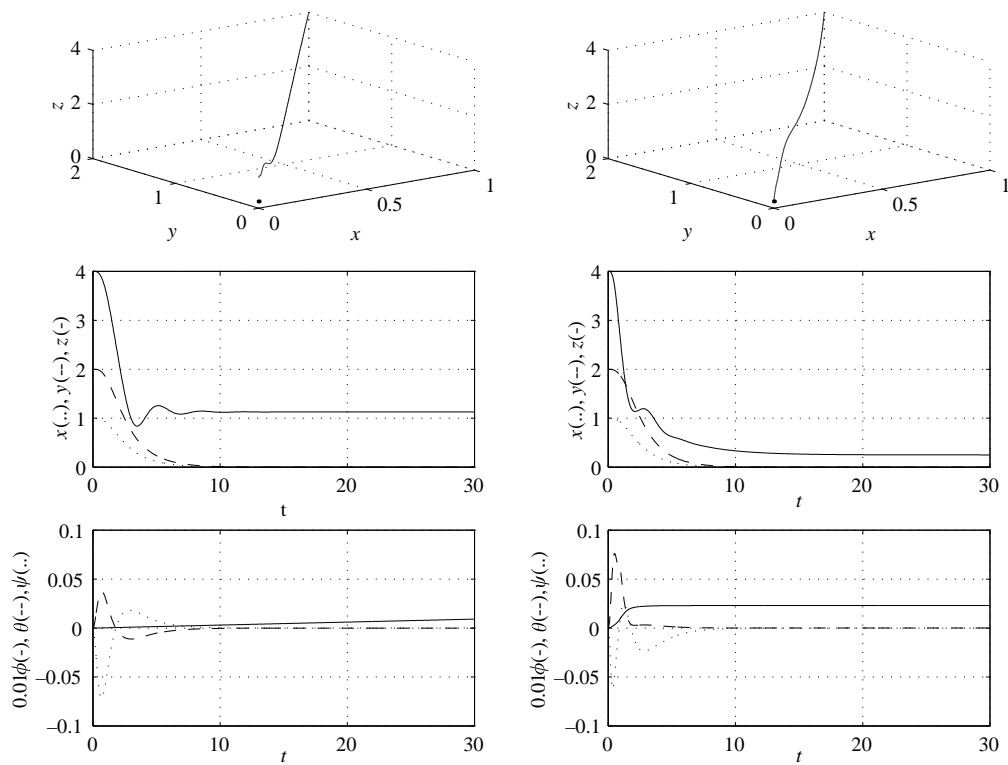


Fig. 4. Evolution of the system states for the proposed closed loop system during a landing manoeuvre where the parametric error

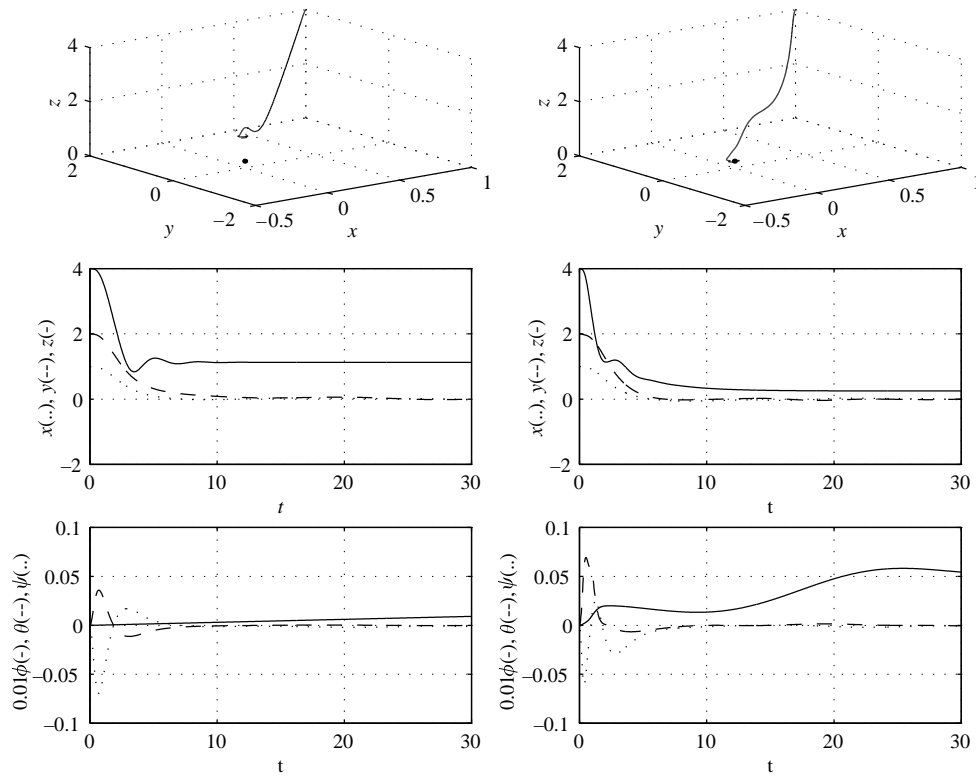


Fig. 5. Evolution of the system states for the proposed closed loop system during a landing manoeuvre in the presence of changes in the lift coefficient due to ground effects, unmodelled dynamics and input noise. Non-adaptive algorithm shown on left versus adaptive algorithm shown on right.

roll (pitch) dynamics with latitudinal (longitudinal) linear dynamics corresponds to the form used in contemporary works [10,12,29]. The noise-like disturbance added to the torque control was chosen to reflect the sort of disturbance encountered due to vortex and dynamic effects that disturb the orientation of the main rotor disk as a helicopter flies close to the ground. The important disturbances tend to be low frequency perturbations as gusts and vortices enter the rotor inflow and cause a bias in the set point regulation for the low level control used to regulate the torque control. The ‘noise’ added was of the form $\nu(t) := 0.05(\cos(t/10)\sin(t/5), \cos(t/5)\sin(t/10), 0)$ to simulate the low frequency aspects of the disturbances and provide a deterministic repeatable noise sequence. High frequency noise effects are filtered by the system dynamics and do not significantly affect the performance of the control algorithm. It should be noted that this ‘noise’ propagates directly into the linear dynamics via Σ . Regarding Fig. 5 it is clear that the proposed adaptive algorithm is stable despite the presence of the added disturbances. Comparing Figs 4 and 5 it may be seen that the added disturbances do not qualitatively degrade the performance of the algorithm. Finally, by regarding the evolution of the parameter

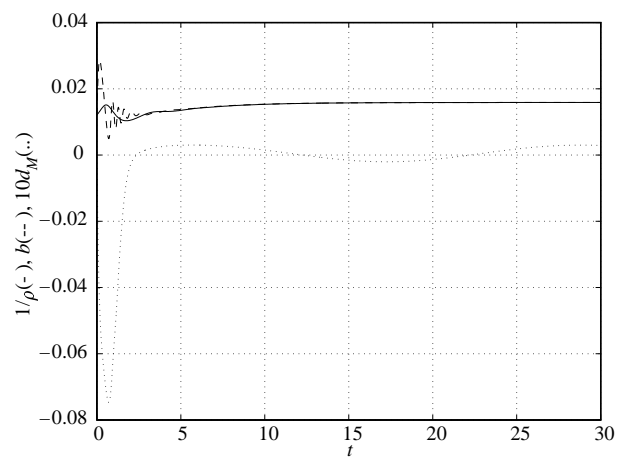


Fig. 6. Evolution of the parameter estimates for the proposed closed loop system (with no trajectory initialisation or σ -modification) during a landing manoeuvre in the presence of changes in the lift coefficient due to ground effects, unmodelled dynamics and input noise.

estimates (Fig. 6) one sees that effective tracking is maintained at all times after a short transient due to the large initial error in the Lyapunov function. The simulation verifies the underlying robustness of the adaptation dynamics.

5. Conclusion

In this paper, we have proposed a simple model for the dynamics of a scale model autonomous helicopter that includes rotor dynamics and certain important aerodynamic effects. The unknown constants associated with the aerodynamic modelling are lumped into linear parametric errors in the model and an adaptive control design based on extended matching is derived. A theorem is given proving convergence of all parametric error estimates to zero and simulations are provided as proof of concept.

In the authors opinion the paper provides the first stage of a necessary research direction in the application of adaptive control techniques to control of scale model autonomous helicopters. It should be stressed that lift coefficient b may never be precisely measured and will usually be slowly varying with time. Any high performance control algorithm will need to take account of this variation.

Although the use of engine torque as the principal control input has excellent theoretical properties and reduces control sensitivity, it has two practical disadvantages. There is significant coupling between the rotor dynamics and the airframe yaw dynamics and the reduced input sensitivity may negatively impact on system performance. In practice, it may be preferable to use an affine approximation of the relationship between thrust and collective pitch [22, Fig. 1.9] and derive an adaptive control to estimate the slope and offset of this approximation on-line. It is the authors opinion that such a formulation of the system will be amenable to the same techniques presented in this paper.

References

1. Amida O. An autonomous vision-guided helicopter. PhD thesis, Electrical and Computer Engineering Department, Carnegie Mellon University. August 1996
2. Bradley R. The flying brick exposed: nonlinear control of a basic helicopter model. Technical Report TR/MAT/RB/6, Department of Mathematics, Glasgow Caledonian University, Scotland, UK. 1996
3. Frazzoli E, Dahleh M, Feron E. Trajectory tracking control design for autonomous helicopters using a backstepping algorithm. In: American control conference, Chicago, IL, USA, 2000
4. Gaonkar GH, Mitra AK, Reddy TS, Peters SA. Sensitivity of helicopter aeromechanical stability to dynamic inflow. *Vertica* 1982; 6(1): 59–74
5. Ghanadan R. Nonlinear control system design via dynamic order reduction. In: Proceedings of the conference on decision and control. Florida, USA, 1994. pp 3752–3757
6. Hauser J, Sastry S, Meyer G. Nonlinear control design for slightly non-minimum phase systems: Applications to v/stol aircraft. *Automatica* 1992; 28(4): 665–679
7. Ioannou I, Kokotovic P. Adaptive systems with reduced models. Springer-Verlag, New York, NY, USA, 1983
8. Kanellakopoulos I, Kokotovic P, Morse A. Systematic design of adaptive controllers for feedback linearizable systems. *IEEE Trans Autom Control* 1991; 36: 1241–1253
9. Kanellakopoulos I, Krstic M, Kokotovic P. Trajectory initialisation in adaptive nonlinear control. In: Proceedings of the 1993 IEEE Mediterranean symposium on new directions in control theory. Chania, Greece. 1993
10. John Koo T, Sastry S. Output tracking control design of a helicopter model based on approximate linearization. In: Proceedings of the IEEE conference on decision and control CDC'98. 1998
11. Krstic M, Kanellakopoulos I, Kokotovic PV. Non-linear and adaptive control design. American Mathematical Society, Providence, Rhode Island, USA, 1995
12. Liceaga-Castro E, Bradley R, Castro-Linares R. Helicopter control design using feedback linearization techniques. In: Proceedings of the 28th conference on decision and control, CDC'89. Tampa, FL, USA. 1989. pp 533–534
13. Loria A, Panteley E, Teel A. A new notion of persistency-of-excitation for UGAS of NLTV systems: application to stabilisation of nonholonomic systems. In: Proceedings of the European control conference, ECC'99. Karlsruhe, Germany. 1999
14. Mahony R, Hamel T, Dzul A. Hover control via approximate lyapunov control for a model helicopter. In: Proceedings of the 1999 conference on decision and control. Phoenix, Arizona, USA. 1999
15. Mahony R, Lozano R. (Almost) exact path tracking control for an autonomous helicopter in hover manoeuvres. In: International conference on robotics and automation, ICRA2000. San Francisco, California, USA. 2000
16. Mallhaupt P, Srinivasan B, Levine J, Bouvin D. A toy more difficult to control than the real thing. In: Proceedings of the European control conference. CD-ROM Brussels, Belgium. July 1997. Version
17. Martin P, Devasia S, Paden B. A different look at output tracking: control of a VTOL aircraft. *Automatica* 1996; 32(1): 101–107
18. Morris J, van Nieuwstadt M, Bendotti P. Identification and control of a model helicopter in hover. In: Proceedings of the American control conference. 1994. pp 1238–1242
19. Murray R, Rathinam M, van Nieuwstadt M. An introduction to differential flatness of mechanical systems. In: Proceedings of Ecole d'Eté, Théorie et pratique des systèmes plats. Grenoble, France. 1996
20. Peters DA, HaQuang N. Dynamic inflow for practical applications. *J the American Helicopter Society* 1988; 3(4): 64–68
21. Praly L, Bastin G, Pomet J.-B, Jiang Z. Adaptive stabilization of non-linear systems. Springer-Verlag, Berlin, 1991. pp 347–434
22. Raymond W. Prouty. Helicopter performance, stability and control. Krieger Publishing Company, 1995. (Reprint with additions, original edition 1986.)

23. Schaufelberger W, Geering H. Case study on helicopter control. Invited session in Control of Complex Systems (COSY) Symposium, Macedonia. October 1998
24. Shakernia O, Ma Y, Koo T, Sastry S. Landing an unmanned air vehicle: vision based motion estimation and nonlinear control. *Asian J Control* 1999; 1(3): 128–145
25. Shim H, Koo T, Hoffmann F, Sastry S. A comprehensive study of control design for an autonomous helicopter. In: Proceedings of the 37th conference on decision and control CDC'98. 1998
26. Sira-Ramirez A, Castro-Linares R, Licéaga-Castro E. Regulation of the longitudinal dynamics of an helicopter system: a Liouvillian systems approach. In: Proceedings of the American control conference ACC'99. San Diego, California, USA. 1999
27. Sira-Ramirez H, Castro-Linares R, Liceaga-Castro E. A Liouvillian systems approach for the trajectory planning-based control of helicopter models. *Int J Robust Nonlinear Control* 2000; 10: 301–320
28. Teel AR. A nonlinear small gain theorem for the analysis of control systems with saturation. *IEEE Trans Autom Control* 1996; 41(9): 1256–1270
29. Thomson D, Bradley R. Recent developments in the calculation of inverse dynamic solutions of the helicopter equations of motion. In: Proceedings of the UK simulation council triennial conference. 1987
30. van Nieuwstadt M, Morris J. Control of rotor speed for a model helicopter: a design cycle. In: Proceedings of the American control conference. 1995. pp 688–692
31. van Nieuwstadt M, Murray R. Outer flatness: Trajectory generation for a model helicopter. In: Proceedings of the European control conference (CD-ROM). Brussels, Belgium. 1997
32. Walker DJ, Postlethwaite I. Advanced helicopter flight control using two-degrees-of-freedom H_∞ optimisation. *AIAA J Guidance, Control and Dynamics* 1996; 19(2): 461–468